NASA TECHNICAL MEMORANDUM

NASA-TM-76689 19820014410

NASA TM-76689

STUDIES ON WIND TUNNEL STRAIGHTENERS

F. Schultz-Grunow and K. Wieghardt

Translation of "Untersuchungen ueber die Wirkungsweise des Gleichrichters", Luftfahrtforschung, Vol. 17, No. 3, Mar. 20, 1942, pp. 82-86.

NATIONAL AERONAUTICS AND SPACE ADMINISTRATION
WASHINGTON, D.C. 20546 MARCH 1982

STANDARD TITLE PAGE

1. Report No.	2. Government Accession No.	3. Recipient's Catalog No.
NASA TM-76689		

4. Title and Subtitle	5. Report Date
STUDIES ON WIND TUNNEL STRAIGHTENERS	March 1982
	6. Performing Organization Code

7. Author(s)	8. Performing Organization Report No.
F. Schultz-Grunow and K. Wieghardt, Göttingen, Kaiser-Wilhelm Institute for Flow Research	10. Work Unit No.

9. Performing Organization Name and Address	11. Contract or Grant No.
Leo Kanner Associates Redwood City, California 94063	NASW-3541
	13. Type of Report and Period Covered
12. Sponsoring Agency Name and Address	Translation
National Aeronautics and Space Administration, Washington, D.C. 20546	14. Sponsoring Agency Code

15. Supplementary Notes

Translation of Untersuchungen ueber die Wirkungsweise des Gleichrichters," Luftfahrtforschung, v. 17, no. 3, Mar. 20, 1942, pp. 82-86.

16. Abstract

A report is given on tests using small-scale straighteners. The studies allowed conclusions on the most favorable depth relationships, flow conditions behind the straightener and on the drag.

17. Key Words (Selected by Author(s))	18. Distribution Statement
	Unlimited-Unclassified

19. Security Classif. (of this report)	20. Security Classif. (of this page)	21. No. of Pages	22.
Unclassified	Unclassified	4 orig. transl.	

NASA-HQ

N82-22284#

STUDIES ON WIND TUNNEL STRAIGHTENERS

F. Schultz-Grunow and K. Wieghardt

The Kaiser-Wilhelm Institute for Flow Research,
Goettingen, West Germany

A report is given on tests using small scale straighteners. The studies allowed conclusions on the most favorable depth relationship, the flow conditions behind the straightener and on the drag.

/82*

CONTENTS

I. GENERAL

When developing a new series of tests for processes of boundary layers it turned out that the present knowledge of the effect of straighteners was insufficient. Although every wind tunnel is equipped with a straightener no systematic studies on its most favorable dimensions are known. This is probably due to the fact that straighteners of conventional size and construction are still not adequate for allowing accurate measurements determining the angular deflection from the flow direction by fractions of a degree. They are also too unwieldy for systematic alterations.

---

* Numbers in the margin indicate pagination in the foreign text.

This necessitated small scale tests which proved to be of an essential advantage for the production. The straightener could be drilled out of an entire block and, thus, the maximum possible accuracy could be achieved during the manufacturing of it. A total of seven straighteners were produced from electroplated sheets with parallel planes but of different thickness. The holes were arranged in accordance with Figure 1. The diameter of the holes amounted to 3 mm, the vertical distance between them to 3.5 mm but the horizontal to 2.8 mm only in order to achieve the maximum density of the perforations. Smaller distances between the holes were impossible to produce. The arrangement corresponds to a ratio of the open section to a total of $\varphi = \frac{Q_F}{Q_G} = 0.721$, while conventional execution usually results in a ratio somewhere between 0.85 and 0.95. Below, the ratio $\frac{t}{d}$ between the depth t and the diameter of the hole d is given for the different straighteners studied in the following table of data:

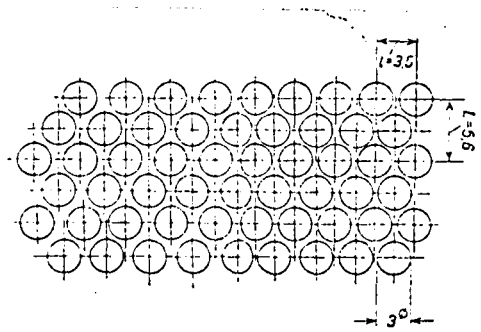

Figure 1. Arrangement of the holes in the straighteners.

Straightener	I	II	III	IV	V	VI	VII
ratio $\frac{t}{d}$	8.33	5	3	1	2:3	1:2	1:6

Nos. VI and VII cannot really be called straighteners, but should rather be termed sieve plate.

II. OBJECT OF THE STUDY

The purpose of a straightener is to make the velocity fields parallel. Basically the present study was aimed at establishing how an airflow hitting a straightener obliquely will be deflected by it. In addition the flow drag was measured and the manner in which the individual air columns emanating from the holes unite to form a homogeneous velocity field was investigated.

III. TEST ARRANGEMENT

During the systematic investigation of the deflecting function the straightener was placed obliquely at certain angles to the airflow from a centrifugal blower and the flow direction behind the straightener was determined.

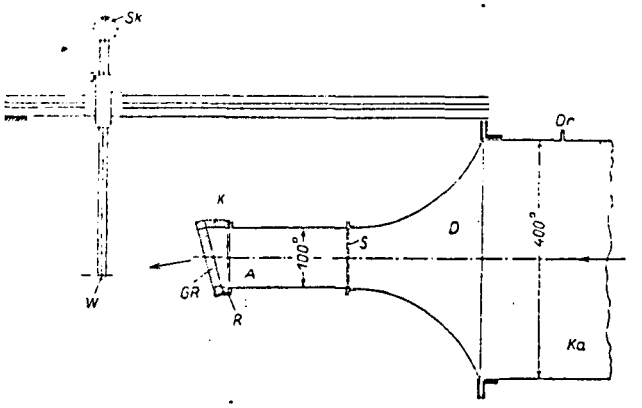

Figure 2. Test arrangement.

The test arrangement can be seen in Figure 2. The air from a blower flows horizontally from the pressure chamber *Ka* (400 · 400 mm) into a square nozzle *D*. A screen *S* and a 200 mm long entrance tube *A* for equalizing the speeds was attached to the nozzle (100 · 100 mm). The edge of the entrance tube was reinforced with a frame *R* so that it formed a solid reference area. To this a wedge-shaped frame *K* was attached and the straightener *GR* fastened with screws to it. The air flowed out into the open through the straightener. By attaching different kinds of wedge-shaped frames the direction of the inflow could be varied.

The outflow direction of the air from the straighteners was measured by means of an angle gauge *W*, described below. In order to measure the direction of the exiting column of air at various positions, the gauge was attached to a sliding mechanism allowing vertical displacement; the sliding mechanism itself was placed on an optically horizontal bench. The measuring positions were at two different distances from the straightener (100 and 200 mm) and at five different points. The angle gauge (Figure 3) consists basically of a /83 cylindrical brass casing, 2 mm in diameter and 100 mm long, which can be rotated around its axis and be inserted perpendicularly to the flow direction. At its rounded tip there are two perforations, 0.2 mm in diameter, forming a 90° angle to each other and connected by separate conduits to a manometer. When the brass casing is rotated so that the pressure in both holes is the same, it means that the air flows symmetrically through both perforations and that the flow direction can be related to the angle of rotation. The angular position

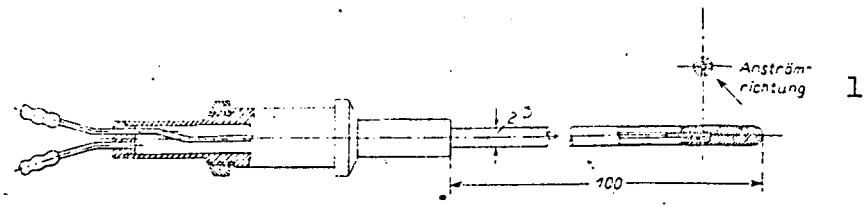

Figure 3. Angle gauge. Key: 1. Oncoming direction of airflow.

of this so-called two-hole gauge can be read at an accuracy of $1/4^{\circ}$ by means of an angle scale (*Sk*) to which a wire leads. This gauge is based on an earlier type suggested by Prandtl and has been used in a similar form by Gruschwitz [1].

IV. EXECUTION OF THE TESTS

a) Angular Measurements

If the flow direction were determined by means of the angle gauge, its position in relation to the straightener surface or to the inflow direction would still not be known since in the outflow direction inaccuracies due to the manufacturing are included such as holes not being drilled at exactly a right angle. The result will depend also on the deviation of the surface of the end-edge level *R* from the vertical in relation to the direction of the inflow. The inaccuracies of the test arrangement could, however, be eliminated by turning the wedge around 180° after measuring an angle so that the airflow became directed upward instead of downward as before and thereafter making a second test and calculating the mean of both measurements.

The angle at which the flow is directed against the straightener, i.e. the angle between the inflow direction and the axis of the holes (in short the "starting angle") is composed of:

1. the wedge angle α_K, and
2. the correction angle $\Delta\alpha$ resulting from the deviation of the end-edge from the vertical in relation to the inflow direction and from the deviation of the straightener perforations from the vertical in relation to the straightener plane.

According to this the starting angle during the first test is

$$\alpha_1 = \alpha_K + \Delta\alpha.$$

During the second test α_K should be given a negative sign due to the 180° rotation of the wedge so that

$$\alpha_2 = -\alpha_K + \Delta\alpha.$$

On the basis of both these equations the mean starting angle α is obtained by ~~differentiating~~ subtracting:

$$\alpha = \frac{1}{2}(\alpha_1 - \alpha_2) = \alpha_K .$$

The mean angle of deflection β, obtained from both tests, must be related to the mean starting angle which is equal to the wedge angle. This mean can also be obtained by ~~differentiating~~ taking the difference in or subtracting the angular measurements β_1 and β_2:

$$\beta = \frac{1}{2}(\beta_1 - \beta_2).$$

This mean corresponds exactly to the α mean when a linear relation

$$\beta = \frac{\alpha}{c}$$

occurs and it can be approximated if the correcting angle $\Delta\alpha$ is small. That this is the correct procedure can easily be confirmed as follows: on the condition that linearity exists, both tests result in

$$\alpha_K + \Delta\alpha = c\beta_1$$
$$-\alpha_K + \Delta\alpha = c\beta_2$$

from which follows that $$\frac{\beta_1 - \beta_2}{2} = \frac{\alpha_K}{c}$$

and, thus

$$\beta = \frac{\alpha}{c} .$$

Since this linear relationship has almost always been confirmed experimentally, the simple formation of the mean as indicated above is justified.

The results of the tests are reproduced in Figure 4. There the angle of defelction is not β but $\gamma = \alpha - \beta$, i.e. the angle of deflection in relation to the axes of the straightener perforations drawn over the starting angle α. Each point of the measurements represents the mean of 20 individual tests at different positions. The graphs drawn as continuous lines correspond to a Reynolds number $Re = \frac{\bar{u} \cdot d}{\nu} = 4540$ where $\bar{u}$ is the mean flow speed in the

TABLE OF FIGURES

DEFLECTION γ DEPENDING ON STARTING ANGLE α.

1. Re = 4540								2. Re = 7140		
α	$\frac{t}{d}$ = 8,33	5	3	1	2:3	1:2	1:6	α	1	1:2
2°	−0,10	0	−0,14	−0,44	−0,10	+0,40	+0,96	4°	−0,53	+0,20
4°	−0,25	−0,065	−0,15	−0,64	−0,165	+1,185	+2,46	6°	−0,60	+0,42
6°	−0,19	−0,10	−0,255	−1,065	−0,375	+1,595	+3,235	12°	−1,03	+1,06
12°	−0,44	−0,50	−0,565	−1,025	−0,45	+2,65	+6,61			

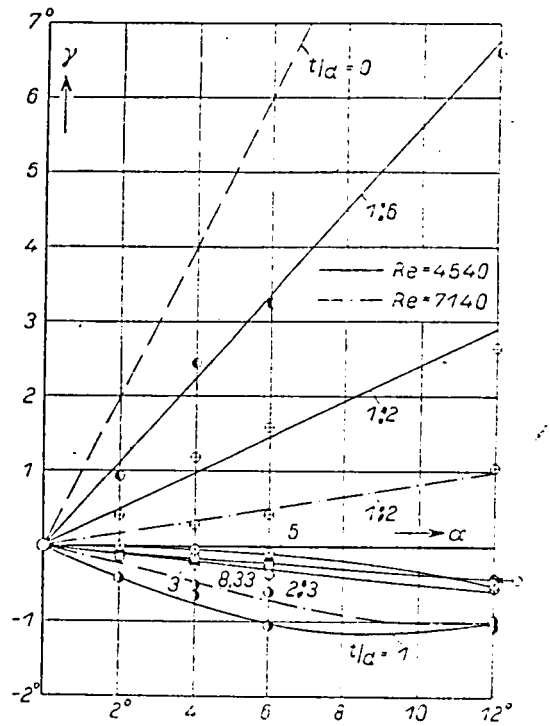

Figure 4. Deflection γ depending on starting angle α.

straightener, ν the kinematic viscosity and d the diameter of the holes. The Reynolds numbers were determined on /84
the basis of the measurements of speed far behind the straightener by dividing the speed obtained there by the above mentioned diameter relation φ. The graphs identified by dash-dot-dash lines were measured at Re = 7140 when testing straighteners nos. IV and VI. For the other straighteners no dependency on the Reynolds numbers could be found within the test range.

Since the measuring points in general confirm the linear dependency it is possible to apply another expression which makes γ dependent on the depth of the straightener. In the case that the linearity is not exact and if the slopes $\frac{\gamma}{\alpha}$ as well as the initial slopes are carried over the depth relationship $\frac{t}{d}$, the graphs will be like those in Figure 5, where $\frac{t}{d} = 0$ corresponds to a value of $\frac{\gamma}{\alpha} = 1$. With increasing $\frac{t}{d}$ the graphs soon begin to dip, reach at $\frac{t}{d} = 0.62$ the zero point and in the vicinity of $1 < \frac{t}{d} < 2$ the minimum value. Approaching the abscissa as far as to $\frac{t}{d} = 5$ they finally move slightly away from it again. No asymptotic value could, thus, be obtained within the test range. The minimum value is lower at a higher Re-number.

It is interesting that the graphs become negative below $\frac{t}{d} = 0.62$. A negative γ angle means that the deflecting effect of the straightener is too strong, i.e. that, for instance, an upward directed input flow will not become horizontal by means of a horizontally adjusted straightener but may even become deflected downward. This excessive deflection will for the sake of brevity be called "superdeflection" below.

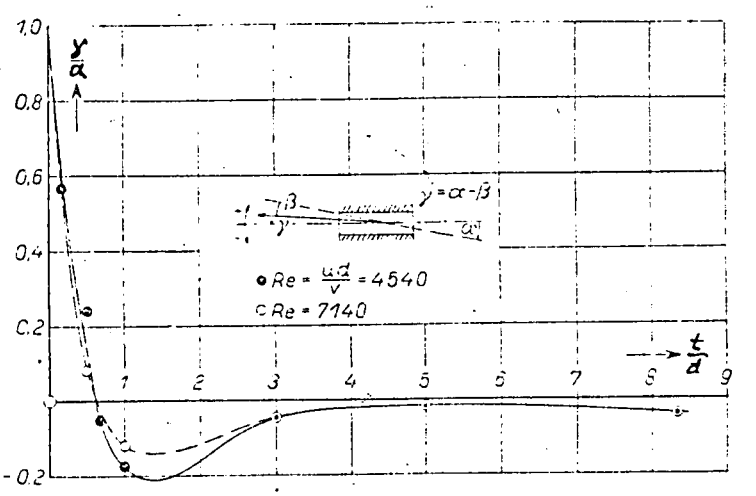

Figure 5. The deflection $\frac{\gamma}{\alpha}$ depending on the depth relationship $\frac{t}{d}$.

An explanation of the assumed development of superdeflection can be seen from the sketch in Figure 6. If the angle at which the air enters a straightener channel is large enough a detachment will occur at the lower rim of the entrance edge. When such a detachment has occurred the airflow will be reaspired to the lower wall of the channel whereby a speed component, directed downward, develops. If the straightener channel ends within that range, the flow will exit with a downward directed component and superdeflection will happen. Furthermore, it is remarkable that superdeflection occurs even under the largest depth conditions investigated. One would rather believe that in long straightner channels the aspiration of the air toward

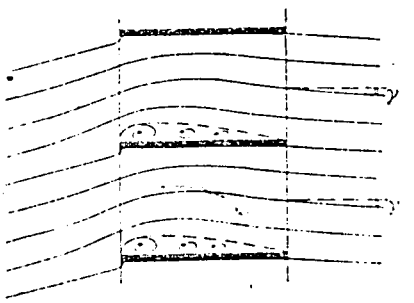

Figure 6. Sketch explaining superdeflection.

the bottom wall of the channel should result in it pulling away from the top wall. It is, however, necessary to reflect on the fact that this explanation takes into consideration neither the secondary flow released due to the detachment nor the pressure field at the exit of the straightener.

The Reynolds numbers affect the deflection only within the range of $\frac{t}{d} < 3$ (Figure 5). This state of the matter is of importance only in so far as it shows that we are within the supercritical range exclusively in the case of rather deep straighteners, i.e. within the area of fully developed turbulence, which is indicated also by the measurements on drag reported below. The reason that the depth of the straightener is of importance here must be looked for in the fact that we are not dealing with a case of fully developed tubular flow for which the flow condition is characterized by the *Re*-number formed on the basis of the tubular diameter, but with a case of inflow for which the determining *Re*-number is based on the length of the inflow.

Finally, it should be noted in respect to these results that they furnish neither any insight into the effect of the opening condition φ nor into that of the relation between the mesh width and the channel diameter [1] in respect to the straightening.

b) Speed Measurements Behind the Straightener

In connection with recent research on the development of turbulence due to screens or grates the velocity fields behind these installations have been given a certain distinction. The grating of a screen divides the homogeneous velocity field into individual columns of air interspersed by wind shadows. Due to the effects of friction and turbulence, the labile distribution breaks down gradually and a homogeneous velocity field is re-established. This transition was the subject of two papers [2, 3] providing conclusions on what laws govern the amplitudes by which the spatial distribution is reduced in relation to the distance from the screen. Both authors found that the amplitude within a certain range of distance diminishes by $1/x$ (x = the distance from the straightener) which agrees with Prandtl's law on the initial manner of blending. While these studies referred to screens, the decline in variation of velocity behind straighteners was investigated here. /85

[1] This ratio has only a value of 0.03 for the straightener and also for the for the blower; for the wind tunnel it amounts to about one third.

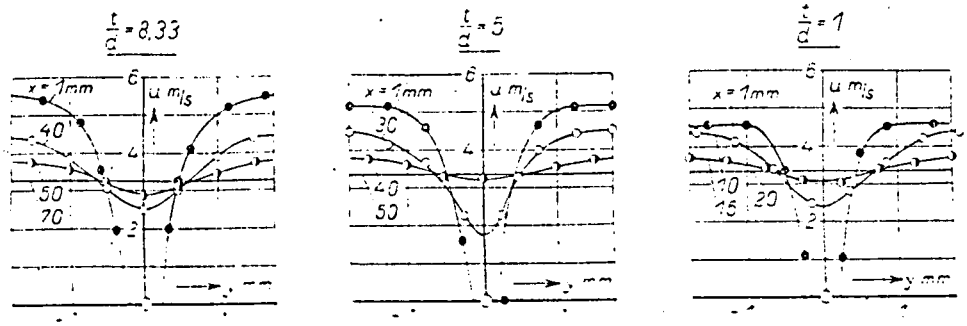

Figure 7. Velocity profiles behind straighteners (Re = 700).

The distribution of velocity at various distances from the straighteners in relation to a vertical row of holes (Figure 1) was measured at the least possible flow velocity, $\bar{u}$ = 4.4 m/s (Re = 724) in order to maintain a laminar flow in the straightener channels. The result is illustrated in Figure 7. In respect to the deepest straightener, no. I, an almost fully developed laminar tubular flow could be observed at the exit from the straightener channel. However, in the case of the other two straighteners there is a nucleus with a constant distribution of velocity. Here we are, thus, still within the inflow area. The deeper straighteners have consequently at their exit a smaller increase in velocity perpendicularly to the flow direction than those less deep.

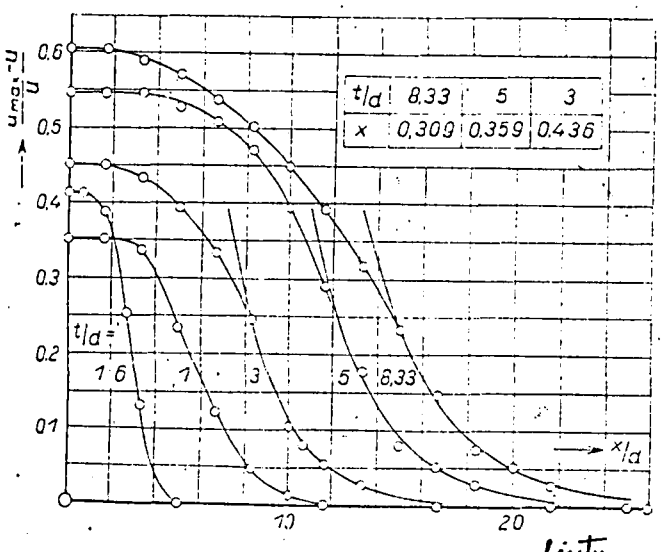

Figure 8. Amplitude of spatial velocity variation depending on the distance from the straightener at Re = 1000.

This difference results in the fact that for the deeper straighteners a homogeneous velocity profile forms only farther downstream than for the shallower ones since the impulse transport causing the equalization is in the case of laminar flow proportional to the increase in speed perpendicularly to the flow direction and in the case of tubular flow proportional to its square.

In Figure 8 the amplitudinal reduction measured is illustrated. The $\frac{u_{max} - U}{U}$ has been drawn over $\frac{x}{d}$ where U is the stationary value of the speed after thorough mixing of

individual columns. The *Re*-number ($Re = \frac{\bar{u} \cdot d}{\nu}$) amounted then to 1000. Since the *Re*-number of a tube is 2800 when affected by a sharp rim, it can be assumed that the flow in the straightener is laminar. The graphs run at first in parallel because the impulse transport has still not penetrated into the nucleus of the columns. As already stated, the deeper the straightener is, the slower the graphs will decline.

The following approximation furnishes some indications regarding the nature of the attenuation. If

$$u = U + u_1$$
$$v = v_1$$
$$w = w_1$$

where U is the speed far behind the straightener, the Navier Stokes equation can be linearized since the interfering speeds of u, v and w are small at a certain distance behind the straightener compared with U:

$$U \frac{\delta u_1}{\delta x} \doteq \nu \Delta u_1.$$

On the basis of the ~~speed~~ velocity profiles shown in Figure 7 it is possible to make the following estimate of u_1 after a certain $\frac{x}{d}$:

$$u_1 = f(x) \cos \frac{2\pi}{l} y \cos \frac{2\pi}{L} z$$

where l and L are the distances between holes in horizontal and vertical direction (cf. Figure 1). After a short calculation, one then obtains:

$$f(x) = c\, e^{-\lambda \frac{x}{d}}, \text{ with } \lambda = \frac{4\pi^2 \nu d}{U} \left(\frac{1}{l^2} + \frac{1}{L^2} \right);$$

the double amplitude $\frac{2f(x)}{U}$ corresponds to $\frac{u_{max} - U}{U}$ in Figure 8. In order to test these data the attenuation graphs in Figure 8 have been approximated by $e^{-\lambda \frac{x}{d}}$ graphs. It then turns out that this kind of attenuation is satisfactorily confirmed by those after $\frac{x}{d}$ where the speed distribution is sinusoidal, while the numerical value of λ will not be correctly reproduced in the above equation.

In addition attemps were made to establish the corresponding ~~speed~~ velocity profiles at elevated *Re*-numbers. The increase in ~~speed~~ velocity perpendicularly to the direction of the flow proved, however, to be too steep to make it possible to establish

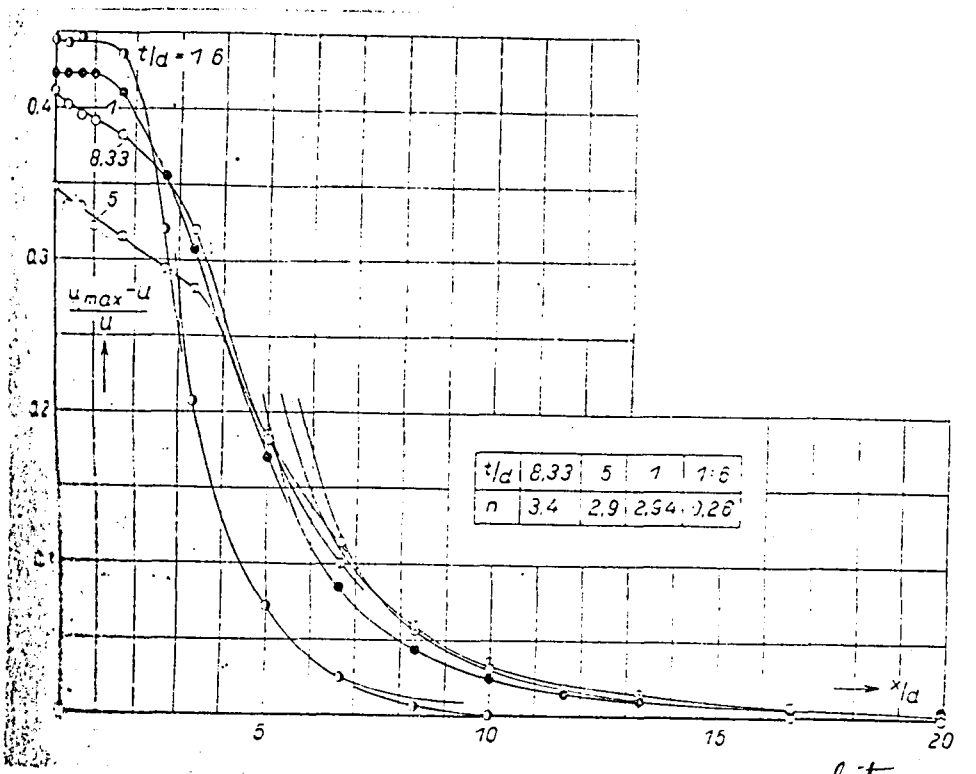

Figure 9. Amplitude of the spatial variations in ~~speed~~ velocity depending on the distance behind the straightener at Re = 7500.

the accurate position during the small-scale tests. Therefore only the maximum value of the ~~speed~~ velocity depending on $\frac{x}{d}$ was measured. During this series of tests the Re-number amounted to 7700, i.e. the flow was turbulent. These measurements are displayed in Figure 9. In comparison with Figure 8 it is worth noting that the graphs here almost agree when the smallest ratio of 1:6, being close /86
to a screen, is not taken into consideration. From a distance of $x = 7d$ the graphs decline almost as $(\frac{x}{d})^{-3}$. An attenuation of $(\frac{x}{d})^{-n}$ at a larger $\frac{x}{d}$ has already been observed for screens. A theoretical explanation can be furnished by an estimate of thrust tension in respect to isotropic turbulence according to Prandtl [4]. The exact powers n for the individual straighteners, obtained by logarithmic ordination, are illustrated in the figure and so are the $(\frac{x}{d})^{-n}$ graphs. The omission of the smallest depth relationship can be explained by the considerably shorter initial distance. It is, thus, evident that for very shallow straighteners the amplitudes diminish much faster than for the deeper and that it is possible to speak of an almost equal regularity of attenuation in the case of the latter. It would be interesting to measure the degree of turbulence as well but because of the small dimensions of the test arrangement, this had to be neglected.

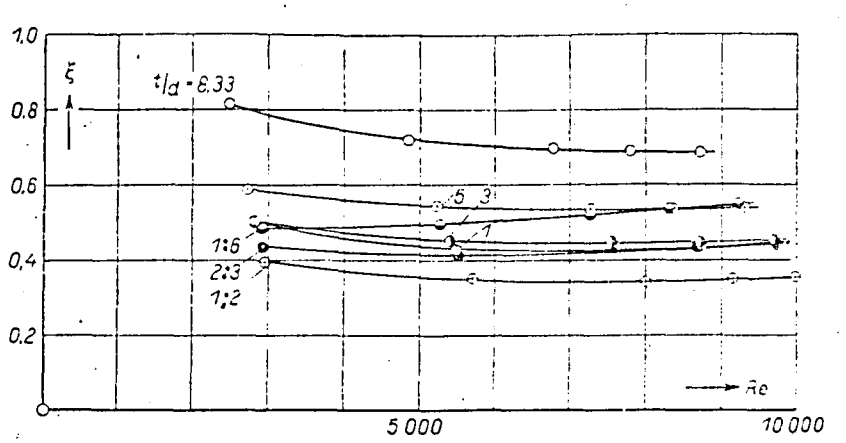

Figure 10. Values of the drag, ξ, depending on the *Re*-number.

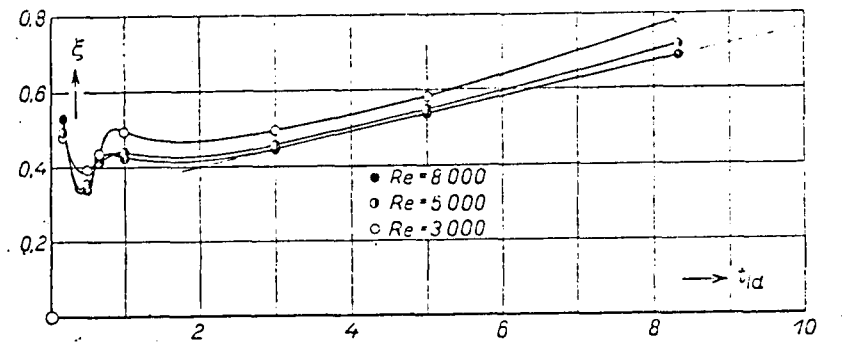

Figure 11. Values of the drag, ξ, depending on the depth ratio $\frac{t}{d}$.

c) Measurements of Pressure Loss

At last we determined also the values of the drag for the different straighteners in order to obtain a fixed point in respect to the pressure loss. The value of the drag can be defined according to the formula:

$$\xi = \frac{p_1 - p_2 + \frac{\varrho}{2}(u_1^2 - u_2^2)}{\frac{\varrho}{2}\bar{u}^2}$$

It relates the total loss of pressure to the mean dynamic damming pressure in the straightener. Here p means static pressure, u the air speed and ϱ the density of the air. Index 1 relates to a section in front of the straightener, index 2 to one placed downstream. During the test the first section was located in

the chamber *Ka* (cf. Figure 1) of the blower where a static pressure bore, *Dr*, was present. Because of the large sectional relationship of the chamber to that of the straightener, u_1 in relation to u_2 can be neglected [$(u_1 : u_2)^2 = 0.004$]. Section 2 was placed 200 mm behind the straightener where the ~~speed~~ velocity field had again become homogeneous. Included in the measurement of the drag is also the energy loss caused by the mixing of the individual air columns. In section 2 only the ~~damming~~ dynamic pressure was measured: the static pressure could be set equal to the ambient pressure. Thus the formula for ξ can be simplified to: DYNAMIC

$$\xi = \frac{p_1 - \frac{\varrho}{2} u_2^2 - \ldots}{\frac{\varrho}{2}\left(\frac{u_2}{\varphi}\right)^2 \ldots}$$

It should be noted that the formula also contains the pressure loss inside the nozzle *D* and the entrance tube *A*. This was, however practically equal to zero so that ξ can be considered the value of the straightener drag alone. The screen *S* was of course removed during these measurements, making it possible to determine separately that an alteration in the inflow due to the removal of the screen had no effect on the value of the drag.

The values of the drag are given in Figure 10 for the different straighteners and drawn in relation to the *Re*-numbers. It turns then out that there is a weak decline in relation to the *Re*-number. The straighteners with the smallest relationships, i.e. nos. V, VI and VII, are an exception in that their drag values increase. This indicates that they are within an area below the critical while the deeper straighteners, at least at high *Re*-numbers, lie within an area below the critical. A satisfactory insight is also furnished by Figure 11, where the values of the drag for the different *Re*-numbers are drawn in relation to $\frac{t}{d}$. Also here the transition area to the supercritical range can be distinctly seen for small $\frac{t}{d}$. It is valid for the supercritical area that the depth relationship is larger than 3 and that the linear dependency is

$$\xi = 0.045 \frac{t}{d} + 0.31.$$

V. CONCLUSIONS

The study of the deflecting effect of a straightener resulted in that the most favorable depth ratio was established to between 5 and 6. The ~~speed~~ velocity

measurements of the outflow allowed conclusions regarding the law of attenuation of spatial variations in speed and the measurements of drag permitted conclusions regarding the dependency of the drag on the depth ration and on the *Re*-numbers.

REFERENCES

1. Gruschwitz, E. "Turbulent friction strata during secondary flow," Ing..-Archiv 6, 355 (1935).
2. Gran Olsson, R., "Speed and temperature distribution behind a screen during turbulent flow," Z. angew. Math. Mechn. 16, 257 (1936).
3. Cordes, G., "Studies on static pressure measurements during turbulent flow," Ing.-Archiv 8, 245 (1936).
4. Prandtl, L. "Contribution to the symposium on turbulence," Proceedings of the fifth international comgress for applied mechanics, p. 340 1938.

Completed May 1939.

End of Document